The roles of pacing interval and pacing strength in ventricular fibrillation induced by rapid pacing with 1 : 1 capture

Dongdong Zhao, Ban Liu, Yidong Wei, Kai Tang, Xuejing Yu, Yawei Xu

Department of Cardiology, the Tenth People's Hospital of Tongji University, Shanghai, China

Submitted: 15 August 2013
Accepted: 22 November 2013

Arch Med Sci 2015; 11, 5: 1111–1118
DOI: 10.5114/aoms.2015.54868

Corresponding author:
Yawei Xu MD
Department of Cardiology
the Tenth People's Hospital
of Tongji University
301 Middle Yanchang Road
Shanghai 200072, China
Phone: 86-21-66306945
Fax: 86-21-66306945
E-mail: zdd808@gmail.com

Abstract

Introduction: The roles of pacing interval (PI) and pacing strength (PS) in ventricular fibrillation (VF) induced by rapid pacing with 1 : 1 capture remain unclear.

Material and methods: Epicardial unipolar electrograms (UEs) were simultaneously recorded using contact mapping in 11 swine. Activation-recovery interval (ARI) restitution was constructed at 4 sites, i.e. the apex and base of the left and right ventricles, respectively. A steady state pacing (SSP) protocol was performed to induce VF. The longest PI and the lowest PS for inducing VF were recorded. Statistical correlation analysis was performed to determine the relationship between local ARI restitution properties and PI and PS for VF induction.

Results: Forty restitution curves were constructed from 11 SSP procedures. The maximal slope (S_{max}) of the ARI restitution curve of the right ventricular apex was positively correlated with the PI for VF induction (r = 0.761, $p < 0.05$). Spatial dispersions of ARI and S_{max} were negatively correlated with the PS for VF induction (r = –0.626 and r = –0.722, respectively, both $p < 0.05$).

Conclusions: Ventricular fibrillation can be induced by rapid ventricular pacing with 1 : 1 capture. The PI for VF induction was related to the S_{max} of the ARI restitution curve of the right ventricular apex, while PS for VF induction was associated with the spatial dispersions of ARI and its restitution property.

Key words: rapid ventricular pacing, electrical restitution, ventricular fibrillation induction, activation-recovery interval.

Introduction

Great interests have been focused on the mechanism of ventricular fibrillation (VF) induction and maintenance in recent years [1–5]. In animal experiments, VF is mainly induced by shock or by rapid pacing [2, 4]. The former was performed by certain strengths of current or by T wave scan to induce VF with single pulse [2, 4], and the VF threshold (VFT) was defined as the minimum strength which could steadily induce VF. The latter was carried out at twice the diastolic threshold with the pacing rate being increased until VF or other ventricular arrhythmias occured [6, 7]. The VFT was defined as the shortest pacing interval which could steadily induce VF.

Ventricular fibrillation induced by rapid pacing has been found to be similar to clinical VF development, but the inducibility is low. Sometimes

1 : 1 capture is lost during rapid pacing and 2 : 1 capture works. The real heart rate at this moment could not exceed half of the pacing rate; thus, VF could not be induced [6, 7]. We have found that when 2 : 1 capture occurred during rapid pacing, 1 : 1 capture can also be recovered by carefully increasing the pacing strength [8]. Then the rapid pacing can be carried on and VF can be induced in most animals [8].

In the new method for VF induction [6–8], both the pacing interval (PI) and the pacing strength (PS) were the necessary factors for VF induction. But their roles may not be the same. In the present study, the roles of PI and PS in the induction of VF were investigated by constructing restitution curves from different epicardial sites using local unipolar electrocardiograms (UEs).

Material and methods

Animal preparation

The protocol conforms to the Guideline for the Care and Use of Laboratory Animals published by the US National Institutes of Health (NIH Publication No. 85-23, revised 1996). Eleven healthy, male pigs (15 ±1.5 kg) were anesthetized with intraperitoneal injection of 0.3% pentobarbital (30 mg/kg), and maintained by isoflurane in 100% oxygen. Body temperature and arterial blood pressure were monitored and stabilized within normal ranges before VF was induced. Surface ECG lead II was continuously recorded during the whole procedure.

The heart was exposed by a median sternotomy, and soaked in warm (37°C) physiological saline intermittently to prevent surface cooling. Two 10-electrode catheters (2-8-2 mm, 6 Fr, Biosense Webster) were sutured to the left and right ventricular (LV and RV) epicardium, respectively (Figure 1 A), to record local UEs. The distal pair of catheters was fixed to the apex, and the proximal pair was attached to the outflow tract (Figure 1 A). A stainless steel needle was inserted into the chest wall subcutaneously as the reference for the mapping electrodes. In each catheter, the 1st and 10th electrode served as the exploring electrodes. Unipolar electrocardiograms were recorded using a digital physiologic recording system (LEAD 2000 B, Jinjiang Inc. China) with a sampling rate of 800 Hz, and were displayed at 100 mm/s screen speed and 10 mm/mV amplitude. A 0.05–500 Hz band pass filter was applied to obtain high quality unipolar signals.

Stimulation protocol

The ventricle was paced at a PS of twice the diastolic threshold via a Teflon-coated bipolar silver needle electrode (2-ms pulse duration) at the epicardium of the right ventricular outflow tract. A dynamic steady state pacing (SSP) protocol was applied to induce VF as previously described [9]. The initial PI was determined by the basic cycle length and maintained for 30 s to achieve a steady state [9]. After each pulse train was delivered, PI was progressively shortened in 20 ms steps for cycle length > 400 ms, in 10 ms steps for a cycle length between 200 ms and 400 ms and in 5 ms steps for a cycle length < 200 ms until 1 : 1 capture was lost. The last PI with 1 : 1 capture at the initial pacing strength was defined as shortest PI. When the shortest PI was reached without inducing ventricular arrhythmias, PS was progressively elevated (by steps of 1 v) to regain the 1 : 1 capture. The dynamic decrease of PI was performed until ventricular arrhythmia was induced. The longest PI and the minimum PS that could steadily induce VF served as a quantitative measurement of VF inducibility.

If VF or VT with hemodynamic deterioration was induced, a 10 to 30-J biphasic DC shock was given (Cardiolife, NIHON KOHDEN) within 1 minute using the defibrillation patches (two pediatric spoon-shaped patches were positioned on the anterolateral wall of the RV and the posterolateral wall of the LV, respectively). If VF was not terminated by a 30-J shock, the pacing protocol was discontinued. However, if VF was terminated by a shock, a 60-minute blank period was given and another SSP protocol was performed as described above.

Signal processing

Local UEs and ECG were replayed at 200 mm/s screen speed and 20 mm/mV amplitude on the computer screen. The waves of the last 5 s of each pulse train were simultaneously recorded for the restitution analysis. Figure 1 B shows a sample of 4 local UEs which were recorded simultaneously. Only waves mapped in 4 sites were measured for constructing the restitution curves, i.e., LV apex (LVA), LV base (LVB), RV apex (RVA) and RV base (RVB). Wave signals between the initial PI and the shortest PI were analyzed. Signals without a smooth and stable diastolic baseline or signals with flat T waves or ST-segment elevation without a clear T-wave upstroke were excluded from this analysis. In each pulse train, at least 5 stable waves were employed and averaged to minimize measurement error. However, when the T wave end was significantly interrupted by the pacing pulse at a rapid pacing rate, only the last paced beat was measured.

Activation-recovery intervals (ARIs) for local UEs represent the time course of repolarization of the intracellular action potential [10, 11]. Using the method described by Lux [12], local activation

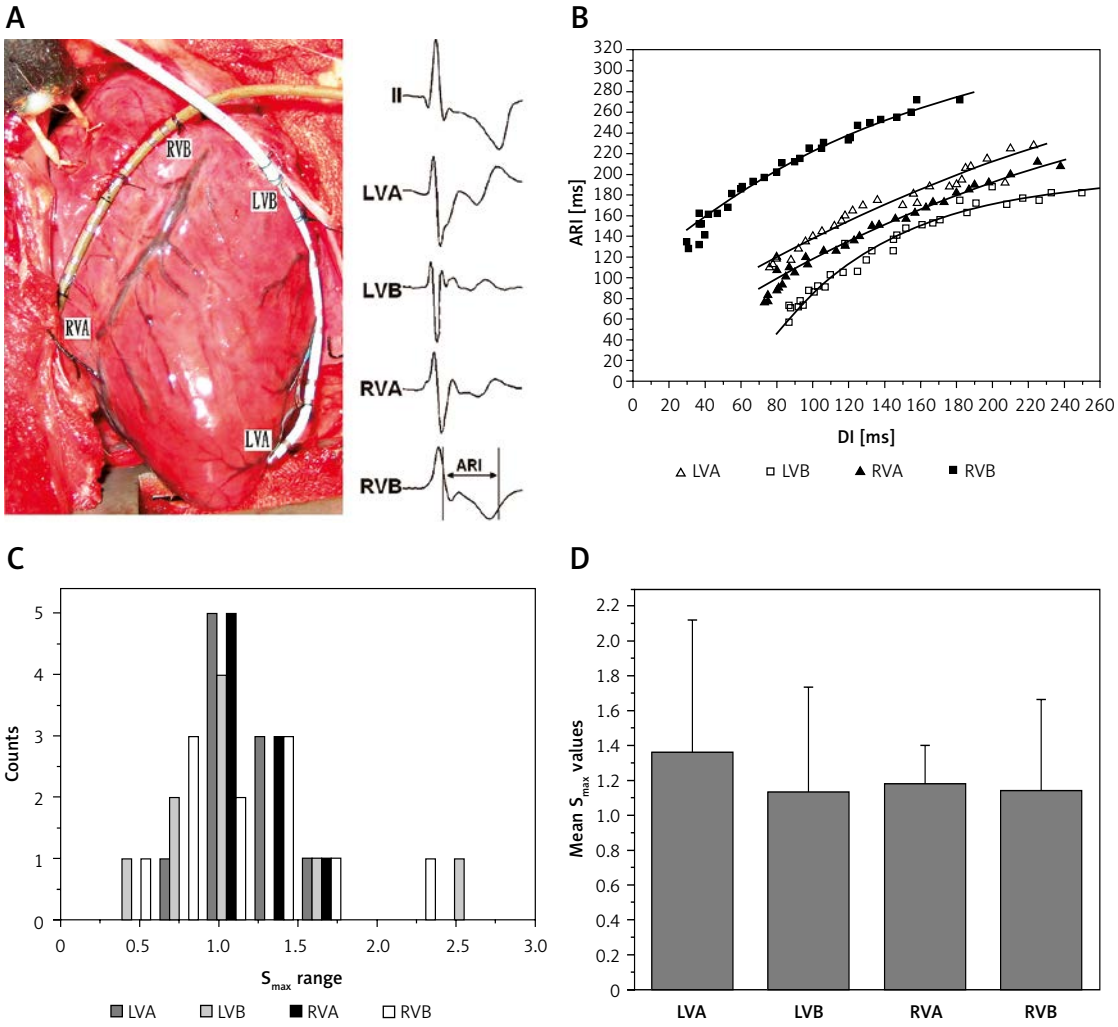

Figure 1. Contact mapping and activation-recovery interval restitution curves in one swine and the distribution of S_{max} at different sites. **A** – Contact mapping was performed in the left ventricular and right ventricular epicardium using two multiple-electrode catheters. Surface electrocardiographic lead II and unipolar electrograms at the apex and base of left and right ventricles were simultaneously recorded. **B** – Activation-recovery interval restitution curves of the 4 epicardial sites. **C** – Frequency counts of S_{max} for restitution curves; the distributions of S_{max} for the restitution curves in 4 different sites were similar. **D** – Mean values of S_{max} for the restitution curves at each site

LVA – Left ventricular apex, LVB – left ventricular base, RVA – right ventricular apex, RVB – right ventricular base, ARI – activation-recovery interval, DI – diastolic interval.

time was defined as the maximum negative slope in the QRS complex (dV/dt min). The repolarization time was defined as the maximum positive slope in the T wave (dV/dt max) [6, 12]. Activation-recovery interval was defined as the interval between activation time and repolarization time (Figure 1 A). Diastolic interval (DI) was defined as the period between the end of repolarization time of the preceding beat and the activation time of the following beat [6, 12]. Activation-recovery interval and DI were measured manually for at least 5 beats at each site during each pacing cycle length, at a recording speed of 200 mm/s, and the mean value of the 5 results served as the true ARI or DI. The spatial dispersion of ARI was defined as the ratio of the spatial standard deviation and the spatial mean, i.e., the coefficient of variation (COV), in percentage [7]. The spatial heterogeneity of ARI was calculated within each animal, and the heterogeneity values of different animals were averaged for comparison.

Restitution curves were constructed by plotting ARI versus DI for local UE recording. An exponential curve (equation 1) using the Levenberg-Marquardt method was used for this analysis [7] (Origin, Microcal Software, Inc):

$$y = \alpha - \beta e^{-x/\tau} \quad (1).$$

With each β and τ, and the DI, the slope was constructed using equation 2:

$$\text{slope} = \beta/\tau * e^{-x/\tau} \quad (2).$$

The maximal slope (S_{max}) of the restitution curve was defined as the slope of the shortest DI of the restitution curve. Figure 1 C shows a sample of 4 ARI restitution curves which were constructed simultaneously.

R^2 is a quantitative value for the degree of fitness of the model. A value close to 1 indicates the best fit. Fitted restitution curves with an R^2 value less than 0.8 were discarded from the analysis.

Statistical analysis

All continuous values were expressed as mean ± standard deviation. Student *t*-test was applied to compare local ARIs and their restitution curve slopes. The nonparametric Wilcoxon signed ranks test was used to compare ranked data. Pearson correlation analysis was applied to detect the correlation relationship of restitution curves S_{max} between two individual mapping sites, and between each recording and PS or PI for VF induction. Value of $p < 0.05$ was considered as statistically significant.

Results

The body temperature was maintained at 36.5 ±1.5°C. There was no significant change ($p > 0.05$) in arterial blood pressure or heart rate during the whole study protocol. The study protocol was completed in all the animals with 11 episodes of VF (Figure 2) being induced. The PIs and PSs for inducing VF were 130–190 ms and 4–10 V, respectively.

Activation-recovery interval and ventricular fibrillation inducibility

Activation-recovery intervals in RV sites were longer than those in LV sites (Figure 3 A, $p < 0.05$ at all PIs). COV_{ARI} was used to quantify the spatial ARI dispersion. No statistical difference was observed between COV_{ARI-LV} and COV_{ARI-RV} (Figure 3 B, $p > 0.05$ at PIs of 350 ms, 300 ms and 200 ms). However, the COV_{ARI} for all the mapping sites was significantly higher than that of LV or RV sites (Figure 3 B, $p < 0.05$ at all PIs). When PI decreased, the mean ARI was shortened but the whole COV_{ARI} was increased (Figures 3 A, B). When compared with the PIs of 300 ms, 350 ms and 400 ms, the whole COV_{ARI} for the PI of 200 ms was significantly larger (p values were 0.016, 0.006 and 0.004 respectively). But COV_{ARI-LV} and COV_{ARI-RV} did not change significantly when the PI altered (Figure 3 B).

Table I shows the associations between COV_{ARI} and VF induction characteristics. None of COV_{ARI-LV}, COV_{ARI-RV} and COV of all sites had a statistical relationship with the PI for VF induction. But COV_{ARI-LV} and COV of all sites were negatively associated with the PS for VF induction ($R = –0.697$, $p = 0.017$ for COV_{ARI-LV} and $R = –0.626$, $p = 0.039$ for COV of all sites, respectively), i.e. the bigger the COV_{ARI-LV} or COV of all sites was, the smaller was the PS need to induce VF. However, no statistical relationship existed between COV_{ARI-RV} and PS.

Local activation-recovery interval restitution properties and ventricular fibrillation inducibility

From 11 SSP procedures, 40 restitution curves for 4 mapping sites were constructed (20 in LV sites, and 20 in RV sites). The mean R^2 value was 0.86 ±0.05. A few restitution curves were discarded due to the low R^2 (less than 0.8, $n = 4$). The restitution curves in each ventricle were variable in their shapes and slopes, and could not be systematically fitted with a simple exponential curve.

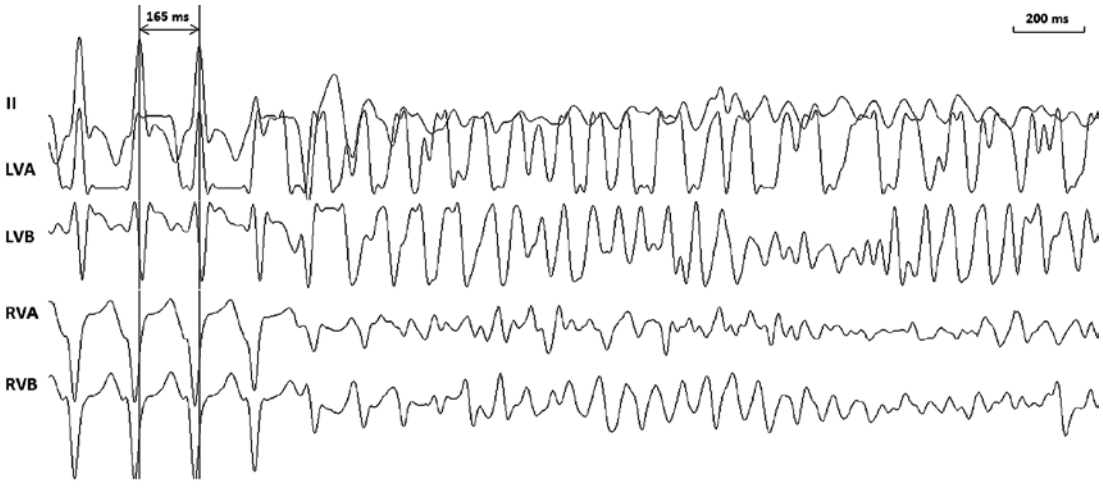

Figure 2. Typical example of ventricular fibrillation induction by steady state pacing in one swine. Surface electrocardiographic lead II and unipolar electrograms at the apex and base of left and right ventricles were simultaneously recorded. The pacing cycle length at which ventricular fibrillation was induced was 165 ms. The pacing strength was 8 V

LVA – Left ventricular apex, LVB – left ventricular base, RVA – right ventricular apex, RVB – right ventricular base.

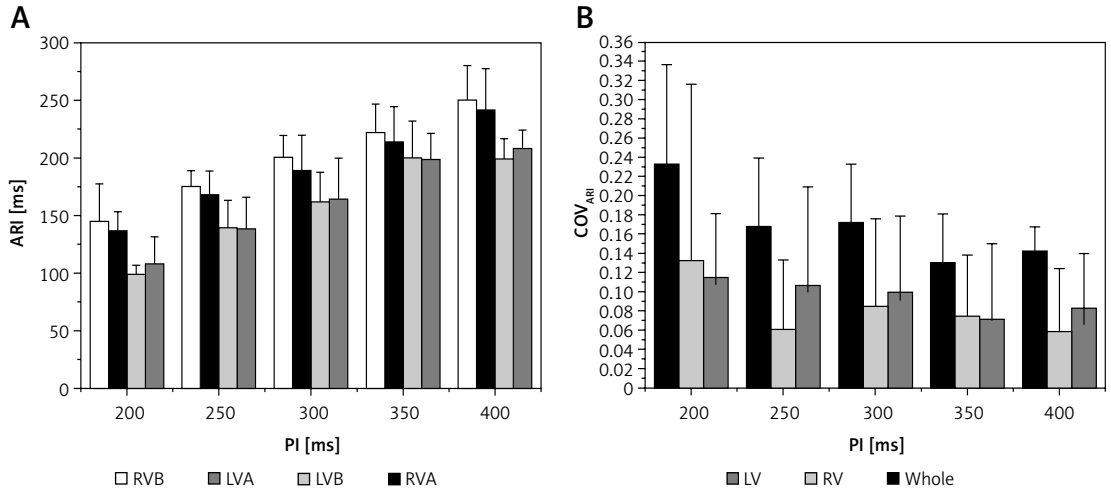

Figure 3. Activation-recovery interval (ARI, **A**) and its spatial dispersion (COV_{ARI}, **B**) during different pacing intervals (PI)

*LVA – left ventricular apex, LVB – left ventricular base, RVA – right ventricular apex, RVB – right ventricular base, COV – coefficient of variation. *P < 0.05 when compared with the values of LV at each corresponding PI; #p < 0.05 when compared with the values of LV or RV at each corresponding PI. See text for detail.*

The S_{max} was not less than 1 in 62.5% of sites (25/40), and the distributions of S_{max} in different value ranges were similar (Figure 1 C). When the mean values of different sites were compared, a regional special difference was rarely noted (Figure 1 D). The mean S_{max} of LV and RV sites was similar (1.21 ±0.51 vs. 1.20 ±0.4, $p > 0.05$). The spatial dispersion of slope (COV_{Smax}) was 0.23 ±0.17 in LV, 0.16 ±0.12 in RV, and 0.20 ±0.15 in all of the mapping sites ($p > 0.05$).

Table II shows the associations between restitution curve slopes and PI or PS for VF induction. Among the regional ARI restitution curves, only the S_{max} of RVA restitution curves was related to the PI for VF induction ($r = 0.761$, $p = 0.028$). None of the local ARI restitution curve slopes had a statistical relationship with the PS for VF induction. COV_{Smax}, both in LV sites and all sites, had a negative relationship with PS for VF induction (Table I). However, there was no statistical relationship between $COV_{Smax\text{-}RV}$ and PS (Table I). There was also no statistical relationship between COV_{Smax} and PI for VF induction (Table I).

Discussion

The major findings in the present study were that: 1) ventricular fibrillation could be steadily induced in swine by rapid ventricular pacing with 1 : 1 capture; 2) the S_{max} of ARI restitution curves

Table I. Associations between COV_{ARI}, COV_{Smax} and VF induction characteristics

		COV_{ARI} (n = 11)			COV_{Smax} (n = 11)		
		LV sites	RV sites	All sites	LV sites	RV sites	All sites
PI	Correlation coefficient	0.014	0.110	–0.106	–0.069	0.101	0.253
	Value of *p*	0.968	0.747	0.757	0.840	0.767	0.453
PS	Correlation coefficient	–0.697	–0.105	–0.626	–0.847	–0.185	–0.722
	Value of *p*	0.017	0.758	0.039	0.001	0.585	0.012

Table II. Associations between local S_{max} and VF induction characteristics

		S_{max}			
		LVA	LVB	RVA	RVB
PI	Correlation coefficient	0.037	0.325	0.761	0.154
	Value of *p*	0.919	0.432	0.028	0.671
PS	Correlation coefficient	0.090	0.440	0.276	–0.108
	Value of *p*	0.792	0.235	0.472	0.752

in RVA was positively related to PI for VF induction; and 3) the spatial dispersions of ARI and S_{max} were negatively associated with the PS for VF induction. These results indicated that PI and PS may play different roles in VF development induced by 1 : 1 capture.

Ventricular fibrillation induction methods

In the present study, we successfully attained VF induction by rapid pacing with 1 : 1 capture in structurally normal swine. Actually, VF can be induced by different approaches such as stimuli on the T-wave [2, 4], rapid burst pacing [6, 7] and direct current pulses. Different modes of VF induction, particularly "shock-induced" compared to "pacing-induced" VF, may result in VF of different characteristics and cycle lengths and may have different defibrillation thresholds. Although idiopathic VF may happen in patients without structural heart disease, VF always occurs in disease-affected heart; thus it is important to realize that many pathological conditions such as the abnormalities of cell-to-cell coupling at the gap junction connexin channels in diseased heart which underlie electrophysiological alterations may promote VF induction and maintenance [13–15]. We used the 1 : 1 capture mode to induce VF mainly due to its high induction rate of VF. With proper PI and PS, VF could be successfully induced in all the swine in our study. Similar results were also obtained in other studies [6, 8]. However, as limited data about VF induction by rapid pacing in humans are available, further studies are needed to clarify whether rapid pacing could also steadily induce VF in humans.

Local activation-recovery interval restitution and the pacing interval for ventricular fibrillation induction

Local electrical restitution can be used to explain the wave break, which results from the aggressive development of alternation [1–4]. Tissue with a steeper restitution curve may result in wave break and act as a "rotor", i.e., the central fibrillation of the heart [1, 16, 17]. The predictive value of local electrical restitution for VF inducibility has been disputed because most of the studies were performed based on mapping of only one or two sites [9, 18–20] and yet the electrical restitutions in different regions may not be the same [19]. In the present study, four sites from the apex and base of LV and RV were mapped simultaneously to construct local ARI levels and the restitution curves. We found that PI and PS, two different factors in VF induction, were associated with local electrical restitutions and the spatial heterogeneity of electrophysiology, respectively.

Associations between local restitutions and PI for VF induction indicate the limitations of using the local restitution property to predict VF. It is assumed that the association between local restitutions and VF is mainly dependent on the VF induction, not on the maintenance. In 1 : 1 capture, with the increment in pacing rate, alternation begins in local sites with steeper restitution curves. When the amplitude of alternations aggressively increases, the wave break will begin. If the micro wavelets resulting from wave break can transmit to other regions, fibrillation will be induced [21].

The mechanism was mainly determined by the status of other tissues around, because the wavelets could disperse throughout the heart only when most other regions were outside the effective refractory period and could be excited. It was confirmed in the present study that only the S_{max} of the RVA restitution curve was related to the PI for VF induction. In the present study, pacing was performed in the epicardium at the right ventricular outflow tract. The tissue at the RVA was excited latest within the RV, and the RVA site was almost the last site to complete the repolarization due to its significantly longer ARI level compared with the LV sites (Figure 3 A). After the RVA completed its action potential, most of the tissues from other areas were already outside the refractory period and could be excited by a premature pulse. If the restitution curve at the RVA site was steep enough to cause wave break, the wavelets would likely be spread to the other areas. Therefore, the restitution property at the site with the latest repolarization throughout the heart seems to be a crucial factor for VF initiation.

COV_{ARI}, COV_{Smax} and the PS for VF induction

The PS has been used to predict VF in many studies, and many theories and hypotheses for VF induction were supposedly based on the spatial dispersion of the effective refractory period [2, 22–25]. The association between PS and the spatial dispersion of ARIs and electrical restitutions was directly confirmed in our study (Table I). However, the statistical association with PS was only found in the spatial dispersion of ARI in LV sites and not in the RV sites. It seems that the spatial dispersion of ARI in the left ventricle is more closely related to VF induction. However, as we only recorded 4 epicardial ventricular sites in our study, the results may not be accurate enough to reflect the spatial dispersion of ventricular electrophysiological properties. Thus, further study is needed to determine whether the spatial dispersion of electrophysiological properties in the LV plays a more important role in VF induction than that in the RV.

No differences of the COV_{ARI}, COV_{Smax} or local S_{max} were noted between LV and RV sites. The only difference between LV and RV was their ARI levels. The RV sites have longer ARIs at all PIs, and the difference increased when PIs decreased. A shorter ARI level, in other studies [26, 27], was proved to cause more complicated characteristics during VF, for instance, more "rotors". Rogers *et al.* [26] and Ten Tusscher *et al.* [27] reported that the fibrillating characteristics of the LV were more complicated than those of the RV. In the present study, the difference in ARI, and the associations of COV_{ARI} and COV_{Smax} with PS for VF induction, also supported the previous findings. It can be supposed that, with a shorter ARI level, tissues in the LV have more complex fibrillating characteristics. The spatial dispersion factors of LV, COV_{ARI-LV} and $COV_{Smax-LV}$ may have strong predictive value for VF inducibility.

In the present study, we only simultaneously mapped 4 epicardial sites. More sites need to be mapped for evaluating the spatial dispersion of restitution properties. Moreover, as transmural dispersion of repolarization was not determined in our study, its role in VF inducibility and maintenance remains unclear. Simultaneous mapping at different myocardial layers will be needed to explore this issue. Third, we only performed ventricular pacing using different PI with a fixed PS (twice the diastolic threshold) at the right ventricular outflow tract, and no different PS was used with a fixed PI at different sites; therefore it remains unclear whether different PSs could lead to higher COV_{ARI} without VF induction. Fourth, as the major purpose of the present study was to investigate the induction characteristics of VF in normal heart for further understanding of the mechanism of VF, the clinical implications of findings in the present study are limited, because the situation of VF in structurally normal heart of humans is not exactly the same as that in the current study.

In conclusion, ventricular fibrillation can be steadily induced by rapid ventricular pacing with 1 : 1 capture in swine in vivo, in which PI for VF induction was related to the S_{max} of the ARI restitution curve of RVA, while PS for VF induction was associated with the spatial dispersions of ARI and its electrical restitution properties.

Acknowledgments

Dongdong Zhao, Ban Liu – these authors contributed equally to this work.

This work was supported by grant 13ZR1432500 (DZ) from Shanghai Natural Science Foundation.

Conflict of interest

The authors declare no conflict of interest.

References

1. Gray RA, Jalife J, Panfilov AV, et al. Mechanisms of cardiac fibrillation. Science 1995; 270: 1222-3.
2. Malkin RA, Idriss SF, Walker RG, Ideker RE. Effect of rapid pacing and T-wave scanning on the relation between the defibrillation and upper-limit-of-vulnerability dose-response curves. Circulation 1995; 92: 1291-9.
3. Weiss JN, Chen PS, Wu TJ, Siegerman C, Garfinkel A. Ventricular fibrillation: new insights into mechanisms. Ann NY Acad Sci 2004; 1015: 122-32.
4. Weiss JN. Ventricular fibrillation: experimental and theoretical developments. Cardiac Electrophysiol Rev 2001; 5: 343-5.
5. Omiya T, Shimizu A, Ueyama T, et al. Effects of isoproterenol and propranolol on the inducibility and frequency of ventricular fibrillation in patients with Brugada syndrome. J Cardiol 2012; 60: 47-54.
6. Cao JM, Qu Z, Kim YH, et al. Spatiotemporal heterogeneity in the induction of ventricular fibrillation by rapid pacing: importance of cardiac restitution properties. Circ Res 1999; 84: 1318-31.
7. Banville I, Chattipakorn N, Gray RA. Restitution dynamics during pacing and arrhythmias in isolated pig hearts. J Cardiovasc Electrophysiol 2004; 15: 455-63.
8. Jiang H, Zhao D, Cui B, et al. Electrical restitution determined by epicardial contact mapping and surface electrocardiogram: its role in ventricular fibrillation inducibility in swine. J Electrocardiol 2008; 41: 152-9.
9. Morgan JM, Cunningham D, Rowland E. Dispersion of monophasic action potential duration: demonstrable in humans after premature ventricular extrastimulation but not in steady state. J Am Coll Cardiol 1992; 19: 1244-53.
10. Yan GX, Lankipalli RS, Burke JF, Musco S, Kowey PR. Ventricular repolarization components on the electrocardiogram: cellular basis and clinical significance. J Am Coll Cardiol 2003; 42: 401-9.
11. Yue AM, Franz MR, Roberts PR, Morgan JM. Global endocardial electrical restitution in human right and left ventricles determined by noncontact mapping. J Am Coll Cardiol 2005; 46: 1067-75.
12. Haws CW, Lux RL. Correlation between in vivo transmembrane action potential duration and activation-recovery intervals from electrograms. Effects of interventions that alter repolarization time. Circulation 1990; 81: 281-8.
13. Fialová M, Dlugosová K, Okruhlicová L, Kristek F, Manoach M, Tribulová N. Adaptation of the heart to hypertension is associated with maladaptive gap junction connexin-43 remodeling. Physiol Res 2008; 57: 7-11.
14. Tribulová N, Knezl V, Okruhlicová L, Slezák J. Myocardial gap junctions: targets for novel approaches in the prevention of life-threatening cardiac arrhythmias. Physiol Res 2008; 57: S1-13.
15. Tribulova N, Seki S, Radosinska J, et al. Myocardial Ca2+ handling and cell-to-cell coupling, key factors in prevention of sudden cardiac death. Can J Physiol Pharmacol 2009; 87: 1120-9.
16. Jalife J. Ventricular fibrillation: mechanisms of initiation and maintenance. Annu Rev Physiol 2000; 62: 25-50.
17. Zaitsev AV, Berenfeld O, Mironov SF, Jalife J, Pertsov AM. Distribution of excitation frequencies on the epicardial and endocardial surfaces of fibrillating ventricular wall of the sheep heart. Circ Res 2000; 86: 408-17.
18. Franz MR, Swerdlow CD, Liem LB, Schaefer J. Cycle length dependence of human action potential duration in vivo. Effects of single extrastimuli, sudden sustained rate ac-

celeration and deceleration, and different steady-state frequencies. J Clin Invest 1988; 82: 972-9.
19. Pak HN, Hong SJ, Hwang GS, et al. Spatial dispersion of action potential duration restitution kinetics is associated with induction of ventricular tachycardia/fibrillation in humans. J Cardiovasc Electrophysiol 2004; 15: 1357-63.
20. Taggart P, Sutton P, Chalabi Z, et al. Effect of adrenergic stimulation on action potential duration restitution in humans. Circulation 2003; 107: 285-9.
21. Lewis TJ, Keener JP. Wave-blocking in excitable media due to regions of depressed excitability. SIAM J Appl Math 2001; 61: 293-316.
22. Behrens S, Li C, Fabritz CL, Kirchhof PF, Franz MR. Shock-induced dispersion of ventricular repolarization: implications for the induction of ventricular fibrillation and the upper limit of vulnerability. J Cardiovasc Electrophysiol 1997; 8: 998-1008.
23. Efimov IR, Gray RA, Roth BJ. Virtual electrodes and deexcitation: new insights into fibrillation induction and defibrillation. J Cardiovasc Electrophysiol 2000; 11: 339-53.
24. Koller BS, Karasik PE, Solomon AJ, Franz MR. Relation between repolarization and refractoriness during programmed electrical stimulation in the human right ventricle: implications for ventricular tachycardia induction. Circulation 1995; 91: 2378-84.
25. Wharton JM, Wolf PD, Smith WM, et al. Cardiac potential and potential gradient fields generated by single, combined, and sequential shocks during ventricular defibrillation. Circulation 1992; 85: 1510-23.
26. Rogers JM, Huang J, Pedoto RW, Walker RG, Smith WM, Ideker RE. Fibrillation is more complex in the left ventricle than in the right ventricle. J Cardiovasc Electrophysiol 2000; 11: 1364-71.
27. Ten Tusscher KH, Hren R, Panfilov AV. Organization of ventricular fibrillation in the human heart. Circ Res 2007; 100: e87-101.